IEEE Access
Multidisciplinary | Rapid Review | Open Access Journal

Received October 13, 2016, accepted October 31, 2016, date of publication November 15, 2016,
date of current version January 4, 2017.

*Digital Object Identifier 10.1109/ACCESS.2016.2629000*

# Hybrid Modeling of Strategic Loading of a Marine Hybrid Power Plant With Experimental Validation

**MICHEL R. MIYAZAKI, ASGEIR J. SØRENSEN, (Member, IEEE), NICOLAS LEFEBVRE, KEVIN K. YUM, AND EILIF PEDERSEN, (Member, IEEE)**

Norwegian University of Science and Technology, Department of Marine Technology, 7491 Trondheim, Norway

Corresponding author: M. R. Miyazaki (michel.r.miyazaki@ntnu.no)

This work was supported in part by the Project Design to verification of control systems for safe and energy efficient vessels with hybrid power plants, where the Research Council of Norway under Grant NFR 210670/070 and Grant NFR 223254/F50, and in part by the Research Council of Norway through the Centres of Excellence under Project 223254-NTNU, AMOS.

**ABSTRACT** Recent developments in marine power systems, energy storage devices (ESDs) technology, and modification to rules and regulations increase the opportunities to improve efficiency and reduce emissions. One particular application is the strategic loading, where the ESD is charged and discharged cyclically, altering the instantaneous fuel consumption, thus aiming to reduce the average fuel consumption. Due to the ESD switching behavior, a hybrid simulation framework is an appropriate dynamic modeling tool. The hybrid simulation model is important in proper design and verification of control strategies for hybrid power plants. A hybrid model was derived, modeling transients as continuous-time events and modeling instantaneous behavior changes as discrete events. Due to the complexity of the system and its hybrid nature (continuous and discrete times), it is important to validate the derived model, such that are known its accuracy and limitations. The developed hybrid model was validated using experiments at the Hybrid Machinery Laboratory, Norwegian University of Science and Technology. The analyzed effects are the steady state, transient behavior, and losses. The transient behaviors include Generator-set (genset) dynamics and load ramps. The losses include the production losses, transmission losses, and ESD losses. The non-modeled effects include the load fluctuation, genset speed variation about the given set-point, and thermal effects on the genset and on the ESD. The results show good correlation between the hybrid model and the experiments. The fuel consumption estimation error stayed below 3% for all 15 analyzed cases, as well as having less than 9% deviation for the $NO_x$ gas emissions estimation. The model is considered as a good approximation for the real operation, enabling its use for design and research purposes.

**INDEX TERMS** Analytic approximations, engine management systems, energy storage, hybrid model, hybrid vehicles, marine systems.

## NOTATION

Throughout this paper, the following notation will be used:

- The subscript "0" refers to the system initial states.
- The subscript "*B*" refers to the ESD system.
- The subscript "*C*" refers to the system while charging the Energy Storage Device (ESD).
- The subscript "*D*" refers to the system while discharging the ESD.
- The subscript "*G*" refers to the system genset.
- The subscript "*L*" refers to the system load.
- The subscript "*max*" refers to the maximum acceptable value for a given variable.
- The subscript "*min*" refers to the minimum acceptable value for a given variable.
- An overline on a variable denotes the average value for that variable.
- The superscript "+" refers to a variable discrete time update (value after a step).

## NOMENCLATURE

| | |
|---|---|
| AC | Alternating Current. |
| *C* | Hybrid system flow set. |
| *D* | Hybrid system jump set. |
| DC | Direct Current. |
| DP | Dynamic Positioning. |
| *E* | Engine. |
| EMS | Energy Management System. |
| ESD | Energy Storage Device. |

| | |
|---|---|
| $F$ | Hybrid system flow map. |
| $f$ | Instantaneous fuel oil consumption. |
| $\dot{f}_{FOC}$ | Instantaneous fuel oil consumption derivative. |
| $FOC$ | Fuel Oil Consumption. |
| $G$ | Hybrid system jump map. |
| Genset | Generator-set. |
| $\mathcal{H}$ | Hybrid system. |
| HML | Hybrid Machinery Laboratory. |
| $M$ | Motor. |
| NOx | Nitrogen Oxides. |
| NTNU | Norwegian University of Science and Technology |
| $P$ | Power. |
| PMS | Power Management System. |
| $s$ | ESD state. |
| $SFOC$ | Specific Fuel Oil Consumption. |
| SOC | State of Charge. |
| SOH | State of Health. |
| SOx | Sulfur Oxides. |
| $x$ | Hybrid system states. |
| $\Delta_C$ | $P_C - P_L$. ESD charging power. |
| $\Delta_D$ | $P_L - P_D$. ESD discharging power. |
| $\eta$ | $\eta_C \cdot \eta_D$. Simplified equivalent efficiency. |
| $\tau$ | Hybrid simulation continuous time. |

## I. INTRODUCTION

Hybrid marine power plants are the state of art for power generation and distribution in the maritime industry. They consist of at least one traditional power producer, such as a diesel genset, or a gas genset, and one ESD, such as batteries, ultra-capacitors, flywheels, etc.

The advantage of having hybrid power plants is its capability to deliver and store energy, and its fast response time. It is possible to operate the gensets with a smooth load demand, or have less gensets connected to the grid, leading to reduced fuel consumption.

Also, it is important to reduce gas emissions, as a result of smoother load demand and set-point changes, specially when it comes to Nitrogen Oxides (NOx) and Sulfur Oxides (SOx) emissions, such that the vessel complies with the environmental requirements posed by [1].

This paper is a direct continuation of the previous initial results published in [2]. Also, it is important to highlight that the term ''hybrid'' is used in two different scenarios in this paper. The first one refers to the ''hybrid'' power plant, where an ESD is added to a conventional marine power plant. The second usage is referring to the ''hybrid'' models, where they consist of a dynamical system with both continuous time and discrete time behavior. It should be clear which denotation is used in each case.

According to recent changes in the rules and regulations of the classification society DNV-GL [3], it is possible, under certain conditions, to utilize an ESD in the same manner as a backup generator. Other classification societies, such as Lloyd's Register and ABS do not have published any clear set of rules for hybrid systems, but have guidelines for hybrid systems and can use it as an alternative to reduce gas emissions.

By disconnecting one of the backup generators, it is possible to reduce the number of engines connected to the grid and increase the average load on the remaining engines, which leads, in general, to a higher genset efficiency. It is known that the diesel/gas engines usually have higher efficiency at higher load.

While hybrid power plants present a potential alternative to reduce emissions and fuel consumption, the lack of rigorous models and analysis tools hinders its usability, since it is dificult to know its behavior and stability without those tools. It is mandatory to develop and validate dynamic models for hybrid power plants which can be used to aid the design process, as well as analyze and optimize during the hybrid power plant operation.

Marine systems are not the only area where hybrid power plants were studied. The automotive industry focused on hybridization by installing fuel cells, ultra-capacitors and batteries to improve the system performance while reducing emissions and fuel consumption. A comprehensive discussion of the different ESD technologies can be found in [4]. Reference [5] presents the effects of hybridization on a conventional diesel bus where the average NOx and fuel consumption were lowered, [6] presents an optimization strategy to minimize the equivalent fuel consumption for a system with a fuel cell where uncertainties are present and discusses the system robustness, and [7] shows an optimization of a Power Management System (PMS) for a real vehicle with a fuel cell/super capacitor hybrid power system, reaching similar fuel consumption levels as a system with more tuning parameters. Finally, a review on the Energy Management System (EMS) for an hybrid vehicle is described in [8].

Some examples out of the automotive industry includes household applications [9], where reduced levels of CO2 emissions were significantly reduced. Cranes, lifts and tooling machines as described in [10], which shows a solution with several benefits over traditional regenerative braking, and [11], where the fuel consumption and emissions were lowered for 35% and 40% respectively.

While examples in other industries were shown with previous references, there are not many researches published on the marine power plants area. Reference [12] reviews the main operations with ESDs in marine power plants, including peak shaving, strategic loading, etc. The strategic loading guidance system continuously cycles the ESD between charging and discharging states, dynamically altering the genset load and consequently the average fuel consumption. It is important to understand the genset characteristics and the ESD characteristics to benefit properly from it, since it might lead to an increase in the fuel consumption and/or pollutant emissions if the guidance system is not planned properly.

Strategic loading has been presented and analyzed in details in previous publications. Reference [13] introduces the strategic loading as well as a comparison between the presented hybrid model and a steady state model,

whereas [2] shows an optimization algorithm based on the steady state model. This paper extends the work presented in [13], to include the hybrid model validation, which was used as a benchmark for the weighted average steady state model presented in it. The hybrid simulation model is important in proper design and verification of control strategies for hybrid power plants.

The modeling framework used to accurately describe the hybrid power plant is *via* hybrid systems modeling, which is a system where variables are both continuous and discrete, being defined as a continuous time system and as a discrete time system, depending on certain conditions. This framework is studied in details in [14]. The main motivation to define the hybrid power plant in the hybrid framework is due to the different time constants of the mechanical system (e.g. engines and generators), and the electrical system (e.g. ESD, breakers). The components with faster dynamics can be modeled as a discrete time action, such as the ESD switching from charging to discharging. On the other hand, mechanical components and power flow are defined in the continuous time frame.

To verify the validity and accuracy of the proposed hybrid models, laboratory experiments were conducted, comparing the simulation results to the real system results. Several experiments were defined, such that as many effects were analyzed independently as possible.

The main contribution of this paper is to derive a hybrid dynamic model of the hybrid marine power plants and validate the model by experiments in the Hybrid Machinery Laboratory (HML) at Norwegian University of Science and Technology (NTNU). Validating a model for strategic loading increases the potential for such strategy to be used in marine hybrid power plants as well as facilitating research on this topic. Moreover, the usage of a hybrid model widens the applications where hybrid systems are used, by applying it in a novel setup.

The paper is organized as follows. An overview of hybrid power plants is given in section II both for Alternating Current (AC) and Direct Current (DC) grids. Section IV presents the hybrid modeling framework as well as how it is applicable to model a hybrid power plant. Section V presents the experimental setup that is used to validate the derived model, which was run in the HML at NTNU. The experiments and results are presented and discussed in section VI. Finally, section VII summarizes the main results and discussions presented in this paper.

## II. HYBRID POWER PLANTS

Marine power plants will differ greatly depending on the vessel type, size, purpose, and operational profile. While many vessels are designed in a manner that it is beneficial to have one main engine mechanically connected to the main propeller, for other vessels it is more interesting to have several gensets generating power, which will be distributed among the many consumers. All electric ships, where no propellers are mechanically connected to the main engine, are mostly common in vessels with Dynamic Positioning (DP) capabilities, Mode details about DP systems can be found in [15].

The DP system will be responsible for keeping the vessel in the desired position/path by using the available thrusters distributed throughout the vessel hull, while minimizing the power consumption. All electric ships will be the focus of this study.

Hybrid power plants are similar to a conventional power plant, with the addition of one or more ESD. The main difference between the ESD and any other element in the power plant is the fact that it can behave either as a generator or as a load, absorbing power and delivering it back to the system when necessary. Fig. 1 shows an example of a hybrid power plant.

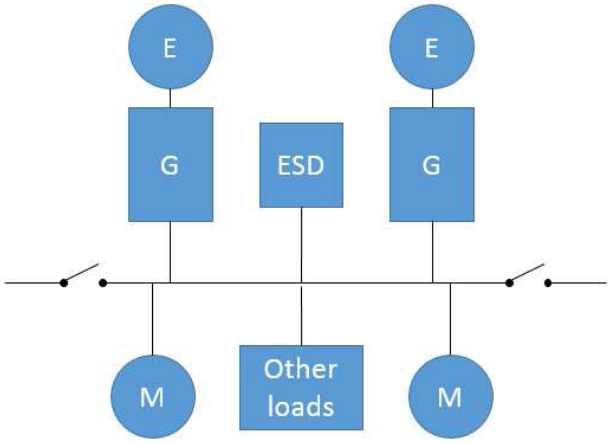


**FIGURE 1.** A hybrid power plant, showing one power bus with two engines, two generators, two motors, one ESD and other loads.

Due to the ESD presence, it is possible to demand a smoother load from the gensets, by having the engine providing a constant power, while the ESD will compensate for the load fluctuation about the average power demand.

Another possibility with hybrid power plants is the fact that the redundancy is increased, since the ESD counts as a backup generator. Thus, it is possible to operate in a DP2 condition [3], while only one genset is connected to the bus, increasing the engine average load, which leads to fuel consumption reduction.

Finally, it is possible to change the system average fuel consumption by cycling the ESD state of charge (charging and discharging it). The idea is to charge the ESD in a condition that will increase the genset efficiency, while reducing the load while discharging the ESD. This method is called strategic loading and will be focused in this study. Strategic loading has a potential to reduce the number of engine running hours, by shutting it down while discharging the ESD as well as reducing the average fuel consumption.

### A. GENERATOR-SET

Gensets are the main source of power in the great majority of marine power plants. They generally are a combination of an engine (typically diesel or gas engines) and a generator.

One important characteristic of the genset is its Specific Fuel Oil Consumption (SFOC). This particular curve presents the fuel consumption (usually in g/kWh) of a particular engine. An example of this curve is shown in fig. 2. This curve is for the Perkins 2506C-E15TAG1 engine which was used in the experiments presented in this paper.

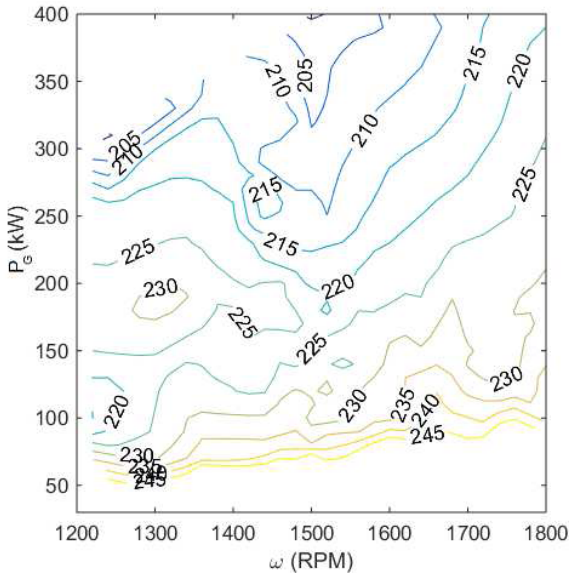


**FIGURE 2.** SFOC curve (in g/kWh) for the Perkins 2506C-E15TAG1 engine, found experimentally at the HML at NTNU.

The SFOC curve has important information about the engine, since it measures its efficiency as a function of the engine speed ($\omega$) and power output (*Power*).

In a case where the engine speed is fixed (most common case for AC grids), the SFOC curve is presented as a single line, such as shown in fig. 3. This specific example presents the same engine, in a condition where the speed is fixed at $\omega = 1500$RPM.

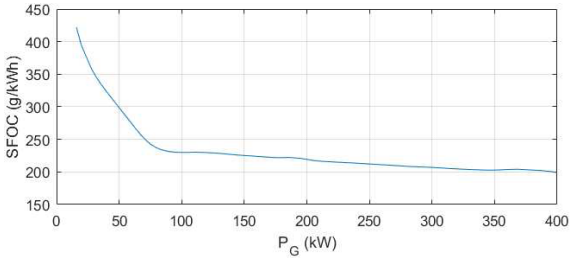


**FIGURE 3.** SFOC for the Perkins 2506C-E15TAG1 engine given that $\omega = 1500RPM$.

Different engines will have different characteristics. For example, the SFOC curve between a gas turbine and a diesel engine will vary, and even among the same technology, it will vary depending on the manufacturer, maintenance, engine size, etc.

### B. ENERGY STORAGE DEVICE

ESD stands for any device capable of absorbing energy and delivering it back to the system on demand. There are several technologies that are useable on a marine power plant, such as batteries, ultra capacitors, flywheels, etc. In this paper, no specific technology is focused on, but instead, parameters common to most ESD are taken into account in the modeling process.

ESDs have several important parameters that affect the system dynamics. Most parameters vary depending on the ESD technology of choice, but the parameters themselves are common factors regardless of the technology.

The data that will be relevant for this study are the maximum stored energy ($E_{MAX}$) in kWh, maximum charge rate ($\Delta_{Cmax}$) in kW, maximum discharge rate ($\Delta_{Dmax}$) in kW, charging efficiency ($\eta_C$), and discharging efficiency ($\eta_D$).

Also, a parameter that has to be kept track over time is the State Of Charge (SOC), which indicates how much energy is stored in the ESD over time. Finally, it is important to keep in mind the ESD State Of Health (SOH), which indicates how the ESD complies according to the manufacturer specification. The SOH decays as it is used, until the ESD has to be replaced.

More details about battery technologies can be found in [16].

### C. POWER GRID

The electrical grid for power distribution consists of the transmission lines (power buses), transformers, breakers, fuses, etc. It comprehends the components responsible for transmitting the power from the producers to the consumers, as well as the safety components.

The transmission lines can operate either in AC or DC.

There are advantages and disadvantages for each option. AC systems have more components, manufacturers, and knowledge available. It is also simpler to implement protection with breakers in AC systems.

AC systems usually control the bus frequency (typically 50Hz or 60Hz) and voltage, as under/over frequency/voltage might lead to power blackout.

Marine DC have lately been more used. On one hand, the components may be more costly, while on the other hand, it is possible to operate the engines in any frequency and there is no problem with synchronization.

More details about electrical grids can be found in [17] and [18].

## III. STRATEGIC LOADING

Strategic loading is a set-point generator that aims to dynamically vary the power produced by the genset in a way that reduces the average fuel consumption and/or gas emissions. The idea is to charge the ESD until it reaches the maximum state of charge set-point ($SOC_{max}$) and then discharge it until it reaches the minimum state of charge set-point ($SOC_{min}$).

The strategic loading will keep repeating the charge/discharge cycles until the operation is interrupted, behaving with a hysteresis in relation to SOC.

Assuming that the average power demanded from the load $P_L$ is constant over time, it is possible to generate a set-point to the genset where it can charge $P_C$ and discharge $P_D$ the ESD. It is necessary that:

$$P_{Gmax} \geq P_C > P_L > P_D \geq 0 \tag{1}$$

Where $P_{Gmax}$ is the maximum rated output from the gensets. Fig. 4 shows an example genset SFOC curve and arbitrary set-points for the strategic loading.

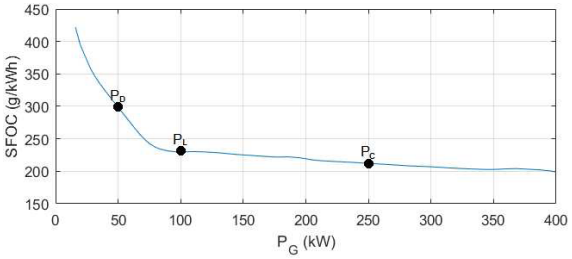


**FIGURE 4.** Example genset *SFOC*, as shown in fig 3, $P_L$, $P_C$, $P_D$ graphical representation in a hybrid system with strategic loading.

The ESD charge rate ($\Delta_C$) and discharge rate ($\Delta_D$) are defined as the difference between the $P_L$ and the genset power output, such that:

$$\Delta_C = P_C - P_L \tag{2a}$$
$$\Delta_D = P_L - P_D \tag{2b}$$
$$\Delta_C \leq \Delta_{Cmax} \tag{2c}$$
$$\Delta_D \leq \Delta_{Dmax} \tag{2d}$$

If the limits in 2 are followed, then the system is able to provide the required power, such that the sum of the gensets maximum rated power plus the ESD maximum output power is greater than the load demanded power ($P_{Gmax} + P_{Bmax} > P_{Lmax}$). Also, there is no restriction on the initial conditions, since it may exceed $\text{SOC}_{min}$ and $\text{SOC}_{max}$, then it will just be charged/discharged accordingly until it is restricted between both values.

The state where the ESD is disabled is not taken into account, since it is not relevant for the strategic loading. Temperature effects are not taken into account, for being considered out of the scope of this study.

## IV. HYBRID MODELING

It is common to distinguish continuous-time systems from discrete-time systems. The hybrid framework combines both methodologies, assuming that a system has a behavior that is characterized by a continuous-time model as well as discrete-time behavior. The way that the simulation evolves can be seen in Fig. 5, where $t$ is the continuous-time and the number of jumps (number of times that the system has a switching behavior) is $j$.

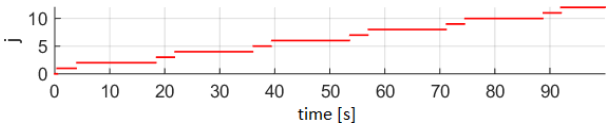


**FIGURE 5.** Representation of the hybrid time $t$ and $j$.

The hybrid system has both continuous-time dynamics and discrete-time dynamics. The continuous-time dynamics (flows) is responsible for the generator speed, load demanded power, etc. The discrete dynamics (jumps) defines the ESD dynamics, when its set-point is switched instantly to a new value, consequently, altering the generator produced power as well. This hybrid model ($\mathcal{H}$) is defined in [14], according to:

$$\mathcal{H} = (C, F, D, G) \tag{3}$$

And the state varies according to:

$$x \in C \quad \dot{x} \in F(x) \tag{4a}$$
$$x \in D \quad x^+ \in G(x) \tag{4b}$$

Where $\dot{x}$ is the states time derivative, $x^+$ is the states time step, $C$ is the flow set, $F$ is the flow map, $D$ is the jump set, and $G$ is the jump map. Both flow and jump sets define the region where the system is flowing or jumping, respectively, while the flow and jump maps define the system behavior inside the respective sets. A system described by (4) can be analyzed for stability according to the framework proposed in (3) and (4).

The hybrid system needs to define several states to properly model the hybrid power plant, such as the generator produced power ($P_G$), the ESD produced power ($P_B$), the demanded load, the ESD state ($s = 0$ when the ESD is discharging and $s = 1$ when the ESD is charging), the ESD SOC, the generator instantaneous frequency ($\omega$), the simulation time ($\tau$), the instantaneous fuel consumption($F$), and the average fuel consumption ($\overline{F}$). All states are described by the state variable ($x$):

$$x = [P_G\ P_B\ P_L\ s\ \text{SOC}\ \omega\ \tau\ \overline{F}\ F]^T \tag{5}$$

Note that the generator speed is not assumed constant, so, transient effects are taken into account. This is to verify the simplified model with the higher fidelity hybrid model and verify the discrepancies between the full analysis and the weighted average static model. The initial conditions, given by the $_0$ subscript are given by:

$$x_0 = \begin{bmatrix} s_0 \cdot P_C + (1 - s_0) \cdot P_D \\ P_{L0} - P_{G0} \\ P_{L0} \\ s_0 \\ \text{SOC}_0 \\ \omega_0 \\ 0 \\ F_0 \\ F_0 \end{bmatrix} \tag{6}$$

The flow map is defined as:

$$f(x) = \dot{x} = \begin{bmatrix} ((s \cdot P_C + (1-s) \cdot P_D) - P_G)/\tau_L \\ \dot{P_L} - \dot{P_G} \\ \dot{P_L} \\ 0 \\ (s \cdot \eta_C + (1-s)/\eta_D) \cdot P_B/E_{max} \\ [s \cdot \omega_C + (1-s) \cdot \omega_D - \omega]/\tau_G \\ 1 \\ [F - \overline{F}]/\tau \\ \dot{f_{FOC}} \end{bmatrix} \quad (7)$$

$\dot{f_{FOC}}$ is the Fuel Oil Consumption (FOC) function time derivative. Eq 7 shows that the genset is modeled as a first order system with time constant $\tau_L$, where the set-point is either $P_C$ or $P_D$, depending on the ESD state. For example, if the system is charging the ESD, the first line results in $\dot{P}_G = (P_C - P_G)/\tau_L$. The genset speed is also considered as a first order system with time constant $\tau_G$, with set points $\omega_C$ and $\omega_D$.

The jump map is defined as:

$$g(x) = x^+ = \begin{bmatrix} P_G \\ P_L - P_G \\ P_L \\ 1 - s \\ \text{SOC} \\ \omega \\ \tau \\ \overline{F} \\ f_{FOC} \end{bmatrix} \quad (8)$$

$f_{FOC}$ stands for the instantaneous FOC value, which is calculated using a look-up table based on $P_G$ and $\omega$, assuming steady-state behavior of the engine.

The flow set is defined as:

$$C = C_1 \cup C_2 \quad (9a)$$
$$C_1 = (s = 0 \ \& \ \text{SOC} \geq \text{SOC}_{min}) \quad (9b)$$
$$C_2 = (s = 1 \ \& \ \text{SOC} \leq \text{SOC}_{max}) \quad (9c)$$

where $C_1$ describes the system while the ESD is being discharged and $C_2$ describes the system while the ESD is being charged. The operator $\cup$ denotes union between two sets and the operator & is the logic operator "AND".

The jump set is defined as:

$$D = D_1 \cup D_2 \quad (10a)$$
$$D_1 = (s = 0 \ \& \ \text{SOC} \leq \text{SOC}_{min}) \quad (10b)$$
$$D_2 = (s = 1 \ \& \ \text{SOC} \geq \text{SOC}_{max}) \quad (10c)$$

where $D_1$ describe the transition from discharging to charging the ESD, and $D_2$ describe the transition from charging to discharging the ESD. Notice that there is a hysteresis when $\text{SOC}_{max} > \text{SOC}_{min}$, thus, no consecutive jumps can occur.

The software flow chart for the developed hybrid system is illustrated in fig. 6

The NOx emissions are calculated in the same manner as $f_{FOC}$, by using a look-up table as a function of the genset output power and speed. The values where found experimentally in the HML at NTNU. Since no other parameters depend on NOx, it was calculated offline, after the simulation was run. The same could be done for $f_{FOC}$, but since it is an essential part of the results, it was decided to include it in the model, calculating it as the simulation is run.

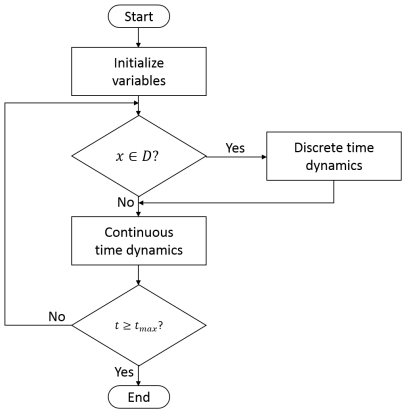


**FIGURE 6.** Hybrid system simulation flowchart.

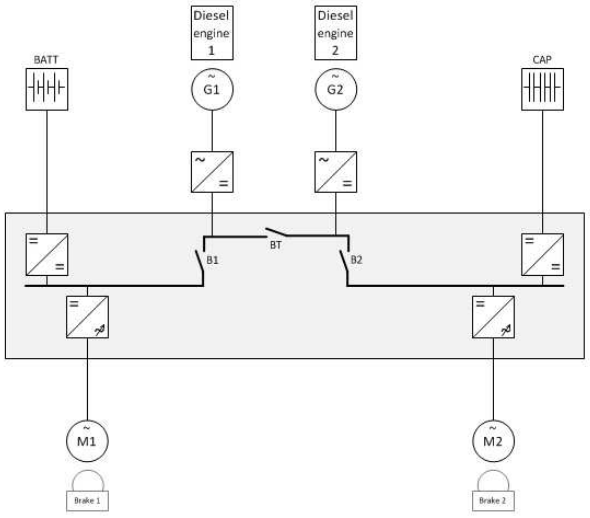


**FIGURE 7.** Single line diagram of the laboratory setup in the HML at NTNU. The power bus is a DC bus, connected to the generators through AC/DC converters, and to the motors through DC/AC converters. There is a battery and an ultra-capacitor connected to the power bus. Figure based on the original presented in [12].

## V. EXPERIMENTAL SETUP

The experiments were conducted at the HML at NTNU, Trondheim. It consists of two diesel engines, connected to DC generators. The DC bus distributes the power to two DC motors connected to brakes. The DC bus is divided in two segments, where each has one engine, one motor and one ESD. Fig. 7 shows the single line diagram of the experimental setup.

Only one genset was used, which is a Perkins 2506C-E15TAG1 engine, retrofitted with the engine

controller from the CAT C15. The reason to substitute the original engine controller is to be able to have a varying speed control in the engine, and consequently a broader operational range. The engine and its corresponding generator are shown in fig. 8.

**FIGURE 8.** Diesel generators of the HML at NTNU, courtesy: ABB.

The engine SFOC curve has been established while considering its power output. In this experiment, it is necessary to calculate the overall system efficiency, which is considered as a constant throughout all simulations.

The eddy current brakes are eddy-current dynamometer WT 470 from Horiba, with a maximum braking capacity of 1000Nm. The brakes are connected to electrical motors, which were set to run at 1500RPM. Motors and brakes are shown in fig. 9. No ESD were physically connected to the system, instead, the engine set-points consider the set-points from the simulation which had the ESD. This simplification is acceptable due to the fact that the ESD time constant is negligible compared to the mechanical system time constant. Also, the ESD low level controller is assumed to be ideal.

**FIGURE 9.** Electric motors and eddy current brakes of the HML at NTNU.

The system is controlled by an ABB PMS, interfaced with a LabVIEW HMI, where the break load set-points are given as well as the engine speed set-point. By setting both the load and the engine speed, it is possible to simulate a realistic operation with variable speed engines.

The system outputs are the DC bus voltage, engine real speed, generator output power, FOC, and NOx.

The NOx emissions are measured by a Horiba Mexa-720. It is given in parts per million (ppm), which is not ideal since it varies with several factors, such as the air temperature and the relative humidity. In the experiments, the ppm is assumed as independent from the remaining factors. There is one correction applied to the NOx measurements, as shown in [19].

It is important to notice that the genset efficiency was found experimentally as 90% and the remaining components in the transmission line have an efficiency around 96%, resulting in a total equivalent efficiency of 87%. Both losses were considered in the simulations to properly compare with the laboratory results.

Another setback with the engine controller that was used was due to the fuel injection. A strategy used by the engine controller is to either have single fuel injection or double fuel injection. The objective of the double injection is to reduce the NOx emissions, in return of an increase of the fuel consumption.

The injection strategy would not be a problem if it was a simple function, that depends only on the generator output power and engine speed, but it is much more complex, having hysteresis as well as depending on several other factors, such as air temperature, humidity, etc. Fig 10 shows part of the injection profile that was found for this specific engine.

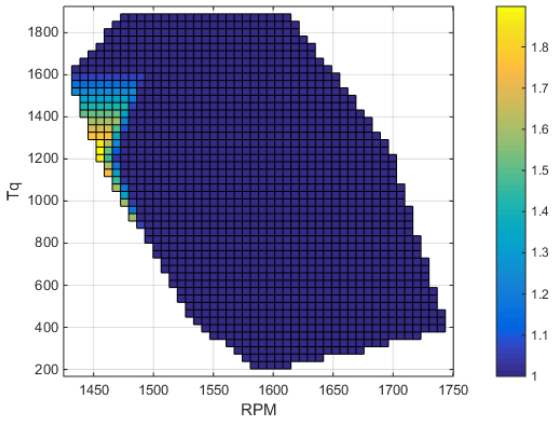


**FIGURE 10.** Average number of injections per cycle on the CAT C15.

It is important to notice that it does not behave in a binary way. Some regions present a combination of single and double injection, making any estimation nearly impossible. Due to those reasons, some experimental points were discarded, since the injection profile did not always match the experimental results. For a more precise NOx estimation, the engine controller injection strategy should be included in the hybrid model.

## VI. EXPERIMENTS

A total 15 experiments were run, separated into 5 different groups of three each. The experiments were grouped in a

**TABLE 1. Experiment fixed parameters.**

| $P_C$ | $P_L$ | $P_D$ | $\text{SOC}_{min}$ | $\text{SOC}_{max}$ | $\text{SOC}_0$ |
|---|---|---|---|---|---|
| 140 kW | 120 kW | 100 kW | 40% | 60% | 60% |

**TABLE 2. Experiment variables.**

| Experiment | 1 | 2 | 3 | 4 | 5 |
|---|---|---|---|---|---|
| $\eta(\%)$ | Variable | 100 | 100 | 100 | 100 |
| $E_{max}$(kWh) | 3 | Variable | 3 | 3 | 3 |
| $\omega$(RPM) | 1500 | 1500 | Variable | 1500 | 1500 |
| $\tau_L$(s) | 10 | 10 | 10 | Variable | 10 |
| $N_A$(kW) | 0 | 0 | 0 | 0 | Variable |

way that all variables but one are kept constant, leading to an isolation of the effects of that specific variable, given the system setup.

Several parameters were fixed for all experiments, and are summarized in table 1. The remaining variables are shown in table 2.

The experiments varied 5 major variables, being the ESD efficiency ($\eta$), the ESD maximum capacity ($E_{max}$), genset angular speed ($\omega$), the load time constant ($\tau_L$), and the noise amplitude ($N_A$), such that:

For each experiment, the engine runs for 1 minute without any load, then, it ramps to the initial value in a linear interpolation for 1 minute, and stays at the initial load level for 5 minutes. After 5 charge/discharge cycles, the load is held at the final value for 5 minutes and ramps linearly to zero during 1 minute interval.

The main purpose for the regions with constant speed and power is to stabilize the engine temperature as well as being used to find the overall electrical system efficiency.

The generated load profile goal is to include repeatability and steady state, to stabilize the engine transient effects such as temperature variations. For the results, the average of the last three charge/discharge cycles are considered, negating some of the possible transient effects.

### A. EXPERIMENT 1: VARIABLE ESD EFFICIENCY

The first experiment analyzes the effect of the ESD efficiency over the system fuel consumption. The efficiency varies from 100% to 80%.

Fig. 11 shows the inputs and outputs from the simulation and experiments. It is noticeable that the genset is capable of producing the desired power and keep the speed relatively stable, with small oscillations in the speed when the power demand varies.

The FOC instantaneous values are not accurate, since it has large fluctuations. On the other hand, the instantaneous FOC is not important for this practical application, instead, the average value is considered instead.

As mentioned before, for each simulation subset, only the three last cycles are considered and the average value is measured. The analyzed results are shown on top of a shaded area in the plots. The results are summarized in table 3.

The results show that regardless of the ESD efficiency,

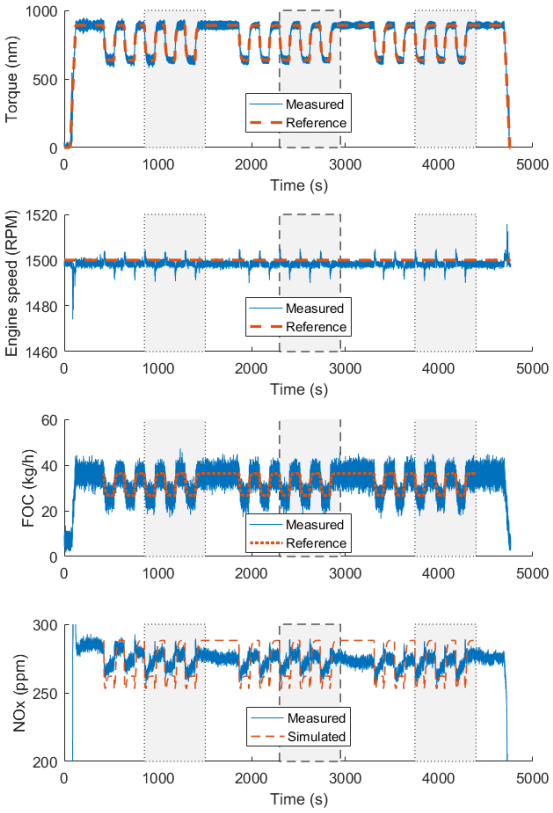


**FIGURE 11. The load profiles applied for each sub experiment. The curves over the shaded background show the cases where the ESD efficiency is $\eta$ = 100%, 90%, and 80% respectively. The first plot presents the total produced power, the second plot shows the engine speed, the third plot shows the resulting FOC, and the final plot presents the resulting NOx emissions for the experiment 1.**

**TABLE 3. Experiment 1 results.**

| Averaged values | $\eta = 100\%$ | $\eta = 90\%$ | $\eta = 80\%$ |
|---|---|---|---|
| $\overline{F}_{exp}$ [kg/h] | 31.5 | 31.7 | 32.0 |
| $\overline{F}_{sim}$ [kg/h] | 31.5 | 31.9 | 32.1 |
| $\overline{F}_{error}$ [%] | 0.03 | 0.21 | 0.07 |
| $\overline{NO_x}_{exp}$ [ppm] | 273.2 | 273.3 | 272.2 |
| $\overline{NO_x}_{sim}$ [ppm] | 270.8 | 271.5 | 272.2 |
| $\overline{NO_x}_{error}$ [%] | 0.88 | 0.66 | 0.04 |

the hybrid model and the experiment present a high correlation, where the largest absolute value in terms of percentage FOC difference between the simulation and experiment was 0.21%. It is important to remember that the error might come from several uncontrollable sources, such as impurities in the fuel, and measurement error. Overall, it is possible to affirm that the hybrid model is a high fidelity description of the average fuel consumption and average gas emissions.

The NOx emission estimation is also a good approximation, where the ESD efficiency did not seem to affect the results. It is important to keep in mind that the NOx measurements are much less reliable than the SFOC, due to sensor deviation and also the fact that the ppm was measured.

Notice that the engine speed drops/overshoots when the

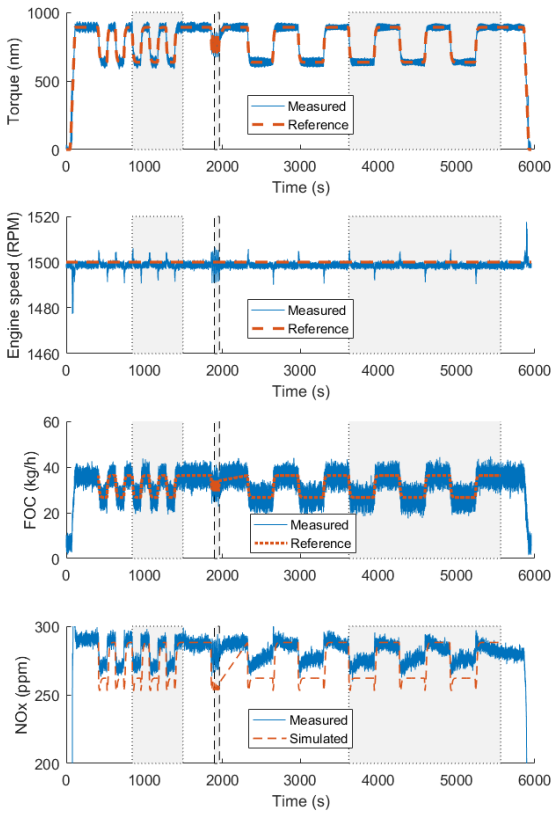


**FIGURE 12.** The load profiles applied for each sub experiment. The curves over the shaded background show the cases where the ESD maximum capacity is $E_{max}$ = 3kWh, 0.3kWh, and 9kWh. The first plot presents the total produced power, the second plot shows the engine speed, the third plot shows the resulting FOC, and the final plot presents the resulting NOx emissions for the experiment 2.

genset load varies. This also affects the fuel consumption and NOx emissions, since the hybrid model does not take into consideration that the genset speed is affected. Also, the genset speed has a slight offset, due to the governor that was used.

### B. EXPERIMENT 2: VARIABLE ESD CAPACITY

Secondly, the effect of the ESD maximum energy capacity is studied, with three different capacities being considered, the maximum capacity selected were 3kWh, 0.3kWh and 9kWh. It is important to notice that the 0.3kWh ESD is so small that the system will not reach the desired $P_C$ or $P_D$ (around 2000s).

Given the fact that the hybrid model and the experiment will switch between charging the ESD and discharge it at the same time, then, if the FOC and NOx emissions mapping are precise enough, both models will have the same FOC and NOx emissions outputs.

Table 4 compiles the results from this experiment, where the hybrid model is accurately describing the average FOC. The maximum error was 0.74%, which is composed by errors in the modeling, measurement noise, etc.

The NOx emission on the other hand, does not present the same degree of precision. The error goes up to almost 9%.

**TABLE 4.** Experiment 2 results.

| Averaged values | 3kWh | 0.3kWh | 9kWh |
|---|---|---|---|
| $\overline{F}_{exp}$ [kg/h] | 31.5 | 31.9 | 31.4 |
| $\overline{F}_{sim}$ [kg/h] | 31.5 | 31.7 | 31.5 |
| $\overline{F}_{error}$ [%] | 0.00 | 0.74 | 0.22 |
| $\overline{NO_{x}}_{exp}$ [ppm] | 280.4 | 279.9 | 279.8 |
| $\overline{NO_{x}}_{sim}$ [ppm] | 270.8 | 255.6 | 273.7 |
| $\overline{NO_{x}}_{error}$ [%] | 3.43 | 8.68 | 2.19 |

**TABLE 5.** Experiment 3 results.

| Averaged values | $\tau_G = 0.1$s | $\tau_G = 100$s | $\tau_G = 10000$s |
|---|---|---|---|
| $\overline{F}_{exp}$ [kg/h] | 30.7 | 30.8 | 31.3 |
| $\overline{F}_{sim}$ [kg/h] | 31.0 | 31.3 | 31.3 |
| $\overline{F}_{error}$ [%] | 1.04 | 1.74 | 2.29 |
| $\overline{NO_{x}}_{exp}$ [ppm] | 320.8 | 305.8 | 303.4 |
| $\overline{NO_{x}}_{sim}$ [ppm] | 317.2 | 308.1 | 310.8 |
| $\overline{NO_{x}}_{error}$ [%] | 1.10 | 0.76 | 2.42 |

As expected, the case where the ESD is smaller has the largest deviations. This is due to transient effects being more dominant. The precision of the NOx emissions can be increased if the NOx mapping is refined, such that it has more data points around the transient areas. Also, it is expected that transient effects will affect the experimental results.

Finally, it is important to point out that the conditions for the first case in this simulation are the same as in condition 2 of experiment VI-C. The FOC estimation is consistent throughout both cases, but the NOx emissions do not present the same degree of repeatability.

### C. EXPERIMENT 3: VARIABLE SPEED

The third group of experiments verifies how the engine speed affects the accuracy of the hybrid model.

This experiment is the only in this paper where the engine speed varies. The engine time constant ($\tau_G$) is set to extreme values, such as 0.1s, where the engine will present high overshoots (around 1000s). On the other extreme, where $\tau_G$ is large, the ESD speed set-point will vary much faster, in a way where the engine speed will not have time to reach it (around 4000s). Table 5 summarizes the results from this experiment.

As expected, the results are not as consistent as before, since unmodeled effects are present in this. One example is the engine speed, which has overshoot, specially for $\tau_G = 0.1s$. On the other hand, the disturbances duration are small, so the variations between the simulated FOC values and the experiments stay between 1.04% and 2.29%.

The NOx emissions also present similar errors to the FOC, up to 2.42%. It is shown that the fast steps do not pose a major setback in the simulations, since it will present a large deviation over a short time period, thus, it will not affect greatly the average values. The major problem with the case where $\tau_G$ = 10000s is the fact that there are few measurement points around this area in the look-up table.

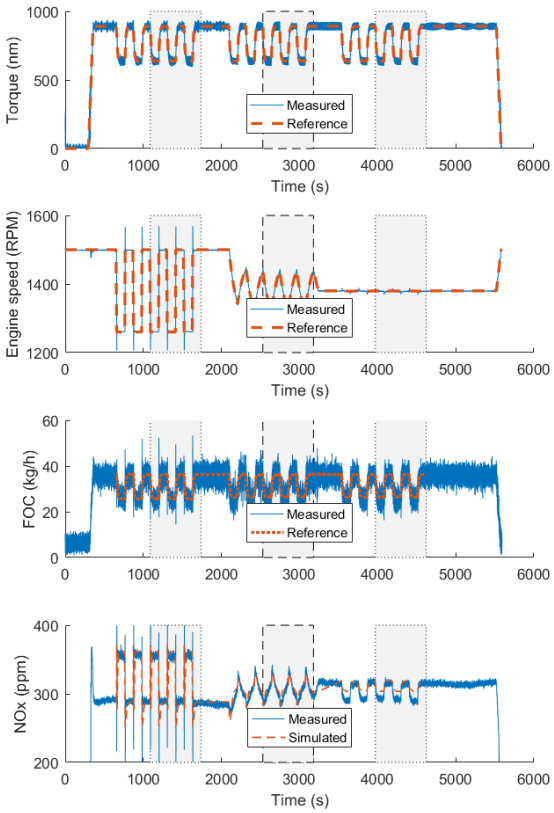


**FIGURE 13.** The load profiles applied for each sub experiment. The curves over the shaded background show the cases where $\tau_G = 0.1$s, 100s, and 10000s respectively. The first plot presents the total produced power, the second plot shows the engine speed, the third plot shows the resulting FOC, and the final plot presents the resulting NOx emissions for the experiment 3.

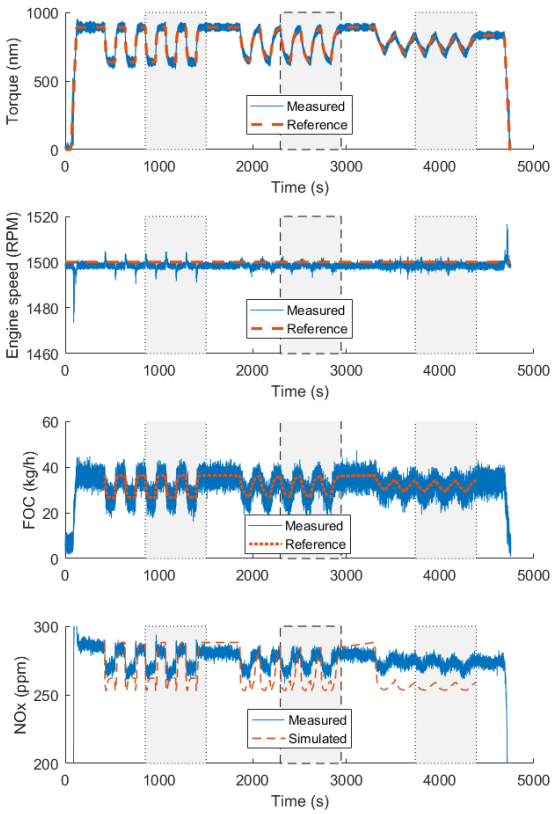


**FIGURE 14.** The load profiles applied for each sub experiment. The curves over the shaded background show the cases where the load time constant is $\tau_L = 10$s, 30s, and 90s respectively. The first plot presents the total produced power, the second plot shows the engine speed, the third plot shows the resulting FOC, and the final plot presents the resulting NOx emissions for the experiment 4.

**TABLE 6.** Experiment 4 results.

| Averaged values | $\tau_L = 10$s | $\tau_L = 30$s | $\tau_L = 90$s |
|---|---|---|---|
| $\overline{F}_{exp}$ [kg/h] | 31.5 | 31.5 | 31.7 |
| $\overline{F}_{sim}$ [kg/h] | 31.5 | 31.6 | 31.6 |
| $\overline{F}_{error}$ [%] | 0.26 | 0.19 | 0.08 |
| $\overline{NO_x}_{exp}$ [ppm] | 275.6 | 274.1 | 272.6 |
| $\overline{NO_x}_{sim}$ [ppm] | 270.8 | 262.7 | 255.6 |
| $\overline{NO_x}_{error}$ [%] | 1.73 | 4.16 | 6.25 |

**TABLE 7.** Experiment 5 results.

| Averaged values | $N_A = 0$kW | $N_A = 2$kW | $N_A = 4$kW |
|---|---|---|---|
| $\overline{F}_{exp}$ [kg/h] | 31.6 | 31.5 | 31.6 |
| $\overline{F}_{sim}$ [kg/h] | 31.5 | 31.5 | 31.5 |
| $\overline{F}_{error}$ [%] | 0.24 | 0.08 | 0.31 |
| $\overline{NO_x}_{exp}$ [ppm] | 272.2 | 271.3 | 269.3 |
| $\overline{NO_x}_{sim}$ [ppm] | 270.8 | 269.3 | 266.4 |
| $\overline{NO_x}_{error}$ [%] | 0.53 | 0.74 | 1.08 |

### D. EXPERIMENT 4: VARIABLE LOAD STEP

Similarly to the analysis of the engine speed effects, the way that the load is applied is analyzed. The model for the load is a first order system with varying time constants. The analyzed time constants were $\tau_L = 10$s, 30s, and 90s.

The results, summarized in table 6, shows that the load time constant will not affect greatly the FOC estimation, since it is a modeled effect in the simulation. The results error stays under 0.3%, which is the second best series of results.

Similarly to section VI-C, the power does not reach a steady state, but instead tends to stay in between the steady states that were presented in VI-A. This also contributes to the results deviation, where a finer experimental mesh can be required.

### E. EXPERIMENT 5: VARIABLE NOISE

The last experiment adds noise to the system, which means that on top of the base switching behavior, a sinusoidal power demand with varying amplitude is added.

The sinusoidal wave function ($y$) is described by:

$$y = N_A \cdot \sin\left(\frac{2 \cdot \pi}{30}\right) \tag{11}$$

The wave period is kept constant as 30s, while the amplitude is variable $N_A = 0$kW, 2kW, and 4kW respectively.

The results for simulation 5 are shown in table 7, where the sinusoidal wave was added on top of the FOC and NOx does not deviate much from the experiments. This is mostly due to the fact that any estimation error is compensated.

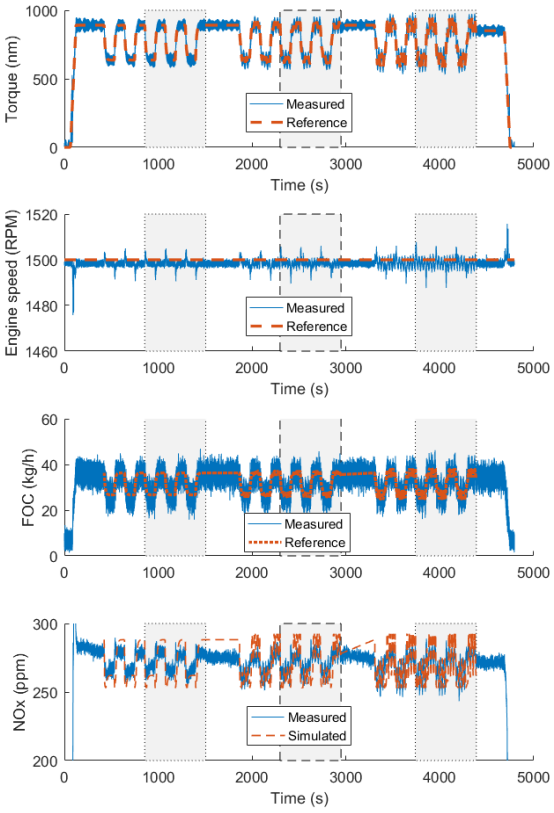


**FIGURE 15. The load profiles applied for each sub experiment. The curves over the shaded background show the cases where the noise amplitude is $N_A$ = 0kW, 2kW, and 4kW respectively. The first plot presents the total produced power, the second plot shows the engine speed, the third plot shows the resulting FOC, and the final plot presents the resulting NOx emissions for the experiment 5.**

For example, if it overestimates the FOC during half of the sinusoidal wave, it will underestimate it on the other half, leading to a good average measurement.

## VII. CONCLUSIONS

This paper showed that the hybrid model for hybrid marine power plants was a good approximation of the real system. The analyzed cases focused on specific aspects of the model, which showed great performance and accuracy, even if transient effects, and efficiency losses were introduced in the system. The FOC estimation error was below 3% and the NOx emission estimation error was below 9%.

The repeatability of the simulations was shown in the initial part of simulations 1 and 2, since both cases had the same parameters. It shows that the FOC estimation is accurate, being repeatable, but the NOx estimation varies among experiments, in this case a difference of about 3%.

As expected, the FOC was estimated more accurately than the NOx emissions, since the latter tended to deviate, even among experiments with the same input parameters.

The emissions were specially affected due to the engine controller, since it has a built in function to include double injection cycles to reduce the NOx emissions. The results can be further refined by studying the injection strategy and/or modeling the engine controller in the model. Also, the number of data points used for the simulation for the NOx and FOC mapping directly affected the model, where a finer mesh will lead to better approximation, but instead will increase the cost required to map it.

Finally, this model was applicable to estimate the average NOx emissions and average fuel consumption, since not all transients are captured by it. Even though the transient effects were not estimated, their effect over the average should be neglectful.

Overall, it was shown that the derived model approximates precisely the experiments, concluding that the hybrid model was a good mathematical approximation of the real system and can be used for further analysis and simulations.

## REFERENCES

[1] *Marine Pollution (MARPOL), Annex VI, The International Convention for the Prevention of Pollution from Ship*, DNV-GL, Høvik, Norway, 2005.

[2] M. R. Miyazaki, A. J. Sørensen, and B. J. Vartdal, "Reduction of fuel consumption on hybrid marine power plants by strategic loading with energy storage devices," *IEEE Power Energy Technol. Syst. J.*, vol. PP, no. 99, pp. 1–11, Jan. 2017.

[3] *Ship Rules for Classification, Ch. 2—Propulsion, Power Generation and Auxiliary Systems*, DNV-GL, Oslo, Norway, Oct. 2015.

[4] C. C. Chan, "The state of the art of electric, hybrid, and fuel cell vehicles," *Proc. IEEE*, vol. 95, no. 4, pp. 704–718, Apr. 2007.

[5] J. Guo, Y. Ge, L. Hao, J. Tan, Z. Peng, and C. Zhang, "Comparison of real-world fuel economy and emissions from parallel hybrid and conventional diesel buses fitted with selective catalytic reduction systems," *Appl. Energy*, vol. 159, pp. 433–441, Dec. 2015.

[6] J. Han, Y. Park, and D. Kum, "Optimal adaptation of equivalent factor of equivalent consumption minimization strategy for fuel cell hybrid electric vehicles under active state inequality constraints," *J. Power Sour.*, vol. 267, pp. 491–502, Dec. 2014.

[7] P. Rodatz, G. Paganelli, A. Sciarretta, and L. Guzzella, "Optimal power management of an experimental fuel cell/supercapacitor-powered hybrid vehicle," *Control Eng. Pract.*, vol. 13, no. 1, pp. 41–53, 2005.

[8] N. Sulaiman, M. A. Hannan, A. Mohamed, E. H. Majlan, and W. R. W. Daud, "A review on energy management system for fuel cell hybrid electric vehicle: Issues and challenges," *Renew. Sustain. Energy Rev.*, vol. 52, pp. 802–814, Dec. 2015.

[9] S. Nižetić, I. Tolj, and A. M. Papadopoulos, "Hybrid energy fuel cell based system for household applications in a mediterranean climate," *Energy Convers. Manage.*, vol. 105, pp. 1037–1045, Nov. 2015.

[10] P. J. Grbović, P. Delarue, P. Le Moigne, and P. Bartholomeus, "The ultracapacitor-based regenerative controlled electric drives with power-smoothing capability," *IEEE Trans. Ind. Electron.*, vol. 59, no. 12, pp. 4511–4522, Dec. 2012.

[11] S.-M. Kim and S.-K. Sul, "Control of rubber tyred gantry crane with energy storage based on supercapacitor bank," *IEEE Trans. Power Electron.*, vol. 21, no. 5, pp. 1420–1427, Sep. 2006.

[12] J. O. Lindtjørn, F. Wendt, B. Gundersen, and J. F. Hansen, "Demonstrating the benefits of advanced power systems and energy storage for DP vessels," in *Proc. Dyn. Positioning Conf.*, 2014, pp. 1–24.

[13] M. R. Miyazaki, A. J. Sørensen, and B. J. Vartdal, "Hybrid marine power plants model validation with strategic loading," *IFAC-PapersOnLine*, vol. 49, no. 23, pp. 400–407, 2016.

[14] R. Goebel, R. G. Sanfelice, and A. R. Teel, *Hybrid Dynamical Systems: Modeling, Stability, and Robustness*, 1st ed. Princeton, NJ, USA: Princeton Univ. Press, 2012.

[15] A. J. Sørensen, "A survey of dynamic positioning control systems," *Annu. Rev. Control*, vol. 35, no. 1, pp. 123–136, Apr. 2011.

[16] D. Linden and T. B. Reddy, *Handbook of Batteries* (Mcgraw-Hill Handbooks). New York, NY, USA: McGraw-Hill, 2002.

[17] P. Kundur, N. Balu, and M. Lauby, *Power System Stability and Control* (EPRI Power System Engineering Series). New York, NY, USA: McGraw-Hill, 1994.

[18] M. R. Patel, *Shipboard Electrical Power Systems* (Shipboard Electrical Power Systems). New York, NY, USA: Taylor & Francis, 2011.
[19] *ISO 8178-1 Reciprocating Internal Combustion Engines—Exhaust Emission Measurement—Part 1: Test-Bed Measurement of Gaseous and Particulate Exhaust Emissions, TC 70 Internal Combustion Engines*, ISO, Geneva, Switzerland, 2006.

**MICHEL REJANI MIYAZAKI** was born in São Bernardo do Campo, Brazil. He received the B.S. and M.S. degree in mechanical engineering from the University of São Paulo, São Paulo, Brazil, in 2010 and 2013, respectively. He is currently pursuing the Ph.D. degree with the Marine Technology Department, Norwegian University of Science and Technology, Trondheim, Norway.

His research topics involves variable speed engines, DC grids, energy storage devices, fuel consumption minimization, and gas emissions reduction.

**ASGEIR J. SØRENSEN** received the M.Sc. degree in marine technology from NTNU, in 1988, and the Ph.D. degree in engineering cybernetics from NTNU, in 1993. From 1989 to 1992, he was at MARINTEK as a Research Scientist. From 1993 to 2002, he was with ABB Group. In 2002, he and his five partners founded Marine Cybernetics AS, where he was the President and the Chief Executive Officer until 2010. In 2012 and 2015, he became a Co-Founder of the NTNU spin-off companies Ecotone AS and Eelume AS, respectively. Since 1999, he was a Professor of Marine Control Systems with the Department of Marine Technology, NTNU. He is currently the Director with the Centre for Autonomous Marine Operations and Systems, Departments of Marine Technology and Engineering Cybernetics, NTNU.

**NICOLAS LEFEBVRE** was born in France in 1977. He received the M.S degree in control theory and design from the University of Technology of Compiègne, France, in 2000, and the Ph.D. degree in optimization and safety system from the University of Technology of Troyes, France, in 2004.

He joined PSA Peugeot Citroën, Paris, in 2000. From 2012 to 2014, he was an Associate Professor with the University of Technology of Troyes, France. Since 2015, he has been with the Norwegian University of Science and Technology, Trondheim, Norway, where he is a Researcher. His main areas of research interest are computer science (artificial intelligence), applied statistics and systems engineering.

**KEVIN KOOSUP YUM** received the B.Sc. degree in naval architecture and ocean engineering from Seoul National University, Korea, in 2001, and the M.Sc. degree in marine engineering from the Norwegian University of Science and Technology in 2012.

He served as an Accounting Officer in the Army of Republic of Korea for 28 months from 2001. He was a Sales Engineer in Samsung Heavy Industries for seven years from 2003. He is currently pursuing the Ph.D. degree in marine engineering since 2012. His main fields of interest are numerical simulation of internal combustion engine system, physical system modeling and technical development and commercial evaluation of LNG cargo handling system and marine system in the ship and offshore unit. In 2015, he was recipient of the Young Scientist Award (second place) in Euro-Korean Conference on Science and Technology.

**EILIF PEDERSEN** received the M.Sc. degree in marine engineering from the Norwegian Institute of Technology, Norway, in 1983. He has been with the Norwegian Marine Technology Research Institute, as a Senior Research Engineer until 1999, where he joined as an Associate Professor. He has held multiple positions, such as a Vice Dean of Education with the Faculty of Engineering Science and Technology, the Head of Master Programs in marine technology, the Leader with the Research Group of Marine Systems, and the Head of Machinery Laboratory with the Department of Marine Technology. He is currently the Leader of the Power Systems and Fuels work package with the Smart Maritime Center for Research-Based Innovation. His areas of expertise are in the field of modeling methodology and simulation of dynamic multidisciplinary and mechatronic systems focusing on machinery system dynamics, internal combustion engines, vibrations, thermal- and hydraulic machines, fuel-cell system dynamics, and hybrid power plants for marine applications.